

Producing a new Fermion in Coherent Elastic Neutrino-Nucleus Scattering: from Neutrino Mass to Dark Matter

Vedran Brdar,^a Werner Rodejohann,^b and Xun-Jie Xu^c

Max-Planck-Institut für Kernphysik, 69117 Heidelberg, Germany

We consider the production of a new MeV-scale fermion in coherent elastic neutrino-nucleus scattering. The effect on the measurable nucleon recoil spectrum is calculated. Assuming that the new fermion couples to neutrinos and quarks via a singlet scalar, we set limits on its mass and coupling using COHERENT data and also determine the sensitivity of the CONUS experiment. We investigate the possible connection of the new fermion to neutrino mass generation. The possibility of the new fermion being the dark matter particle is also studied.

I. INTRODUCTION

Despite being the most elusive Standard Model (SM) particles, neutrinos have been detected in a number of charged- and neutral-current processes. The recent measurement [1] of coherent elastic neutrino-nucleus scattering (CE ν NS) [2–4] yields a novel channel where, for the first time, the interaction of low energy neutrinos with nuclei as a whole is probed. This serves not only as a handle to probe SM and nuclear physics parameters, but also as a robust probe of new physics. In particular, light sterile neutrinos [5–7], non-standard interactions of both quarks and leptons [8–16] as well as neutrino magnetic moments [17, 18] can be searched for.

The basic requirement for the coherent neutrino-nucleus scattering is the smallness of the momentum transfer. Namely, in case it exceeds the inverse size of the nucleus, one can in principle determine on which nucleon the scattering occurred and this is what breaks the coherence. It is also important that the quantum state of the nucleus does not alter in the scattering because, otherwise, the nuclear excitations in such processes would allow individual nucleons to be tagged which would again directly break the condition for the coherent scattering [19].

On the other hand, the production of new light particles does not a priori violate the coherence as long as the above conditions for nuclei are satisfied. Hence, in this work we explore an interesting new possibility for coherent elastic scattering process, namely

$$\nu N \rightarrow \chi N.$$

Here a light MeV-scale fermion (dubbed χ) is produced from the interaction of the incoming neutrino ν with a nucleus N . We are interested, given the lack of evidence for new physics at high energy, in MeV-scale particles as this is the typical energy scale of CE ν NS, where naturally the most interesting phenomenology arises.

Assuming in a minimal setup that the interaction of the new fermion χ with neutrinos and quarks is mediated by a scalar singlet S , we derive limits on the masses of χ and S and their coupling to neutrinos and the nucleus. Existing and expected data from the running experiments COHERENT [1] and CONUS [20] is used, and the results are compared to existing terrestrial and astrophysical limits. In the near future, other upcoming experiments including ν -cleus [21],

^a vbrdar@mpi-hd.mpg.de

^b werner.rodejohann@mpi-hd.mpg.de

^c xunjie.xu@mpi-hd.mpg.de

CONNIE [22], MINER [23], TEXONO [24], ν GEN [25] and Ricochet [26] will also be able to measure the $\text{CE}\nu\text{NS}$ process.

Any new fermion that couples to light neutrinos needs to be considered regarding its role in the generation of neutrino mass, and we demonstrate that a straightforward extension of the type-I seesaw mechanism can indeed generate the observable magnitude of neutrino masses, as well as be testable in $\text{CE}\nu\text{NS}$. Moreover, any new particle beyond the Standard Model is an attractive candidate for dark matter (DM), therefore we investigate in such a setup whether χ can be such a popular MeV-scale DM candidate (see e.g. Refs. [27–32] for recent studies). We find that for the size of the couplings to which $\text{CE}\nu\text{NS}$ experiments are sensitive, the DM abundance can match the observed value in case there was an entropy injection episode between the QCD phase transition and Big Bang Nucleosynthesis (BBN).

The paper is organized as follows. In Section II we derive bounds on the relevant couplings and masses within our framework of $\nu N \rightarrow \chi N$ coherent scattering without restricting the discussion to a specific model. We also obtain the corresponding recoil spectra of N in case a massive particle χ is emitted in the final state. In Section III we discuss a minimal UV-complete setup in which the MeV-scale χ is related to neutrino mass generation. Section IV is devoted to the assumption that χ is the DM particle, in which we scrutinize its production in the early Universe. Finally, in Section V we conclude.

II. PROBING MEV-SCALE PARTICLE IN $\text{CE}\nu\text{NS}$

In this section we investigate the phenomenological aspects of $\nu N \rightarrow \chi N$ coherent scattering by assuming only the following interaction

$$\mathcal{L} \supset y_\chi \bar{\chi} S \nu + y_N \bar{N} S N, \quad (1)$$

where y_χ and y_N parametrize the strength of the Yukawa interaction of a mediator particle S with ν - χ and the nucleus, respectively. In principle, the mediator for a $2 \rightarrow 2$ process with fermions on the external legs can be a scalar or vector boson; we will consider scalar mediators here, though the discussion in Section II A is independent on this. Furthermore, we do not require significant mixing between active neutrinos and χ for coherent scattering, and hence the exchange of SM gauge bosons is suppressed. Model building options for generating interactions of a scalar singlet S with quarks, and hence eventually nuclei, are presented for instance in Ref. [14]. The process under our consideration is shown in a diagrammatic form in Fig. 1.

A. Prerequisites for obtaining the cross sections

Due to the mass of χ , the process $\nu N \rightarrow \chi N$ has different kinematics than $\text{CE}\nu\text{NS}$. Hence, as a starting point, we derive some relations for the kinematics of this process that will be used throughout the paper. The notation of various quantities is given as follows:

- p_1^μ and p_2^μ denote the initial 4-momenta of the neutrino and the nucleus, respectively;
- k_1^μ and k_2^μ denote the final 4-momenta of χ and the nucleus, respectively;
- $q^\mu \equiv k_2^\mu - p_2^\mu = p_1^\mu - k_1^\mu$ denotes the momentum transfer in the scattering process;
- M , m_χ , and m_S denote the masses of the nucleus, χ , and the mediator S , respectively;

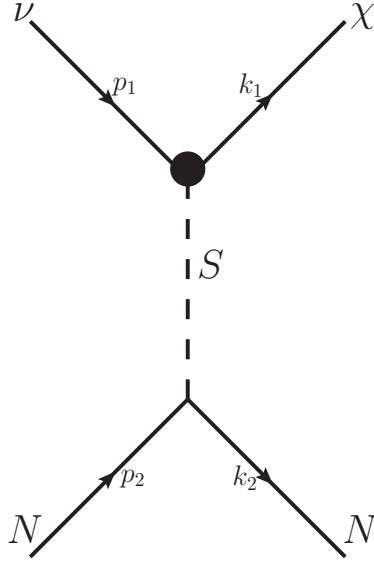


FIG. 1. Feynman diagram for $\nu N \rightarrow \chi N$ coherent scattering mediated by a scalar S . The blob represents the (possibly effective, see Section III A) ν - S - χ vertex.

- E_ν is the energy of the incoming neutrino;
- T denotes the recoil energy of the nucleus, and $p = \sqrt{(M + T)^2 - M^2}$ is the recoil momentum;
- θ is the angle of the outgoing nucleus with respect to the incoming neutrino; i.e. the angle between \mathbf{k}_2 and \mathbf{p}_1 .

Using the above notations, we can explicitly express the 4-momenta:

$$p_1^\mu = (E_\nu, E_\nu, 0, 0), \quad (2a)$$

$$p_2^\mu = (M, 0, 0, 0), \quad k_2^\mu = (M + T, p \cos \theta, p \sin \theta, 0), \quad (2b)$$

$$q^\mu \equiv k_2^\mu - p_2^\mu = (T, p \cos \theta, p \sin \theta, 0). \quad (2c)$$

When computing the cross section, scalar products of the external momenta (e.g. $p_1 \cdot p_2$, $p_1 \cdot k_1$, $p_2 \cdot k_2$, etc.) will be used. All scalar products of p_1^μ , p_2^μ and q^μ (k_1^μ and k_2^μ can be expressed in terms of these three 4-momenta) read:

$$\begin{aligned} p_1^2 &= 0, & p_2^2 &= M^2, & q^2 &= -2MT, \\ p_1 \cdot p_2 &= ME_\nu, & p_1 \cdot q &= -MT - m_\chi^2/2, & p_2 \cdot q &= MT. \end{aligned} \quad (3)$$

We obtained q^2 by squaring both sides of $q^\mu \equiv k_2^\mu - p_2^\mu$ and using Eq. (2b):

$$q^2 = k_2^2 + p_2^2 - 2k_2 \cdot p_2 = 2M^2 - 2M(M + T) = -2MT.$$

Applying the same to $p_2^\mu + q^\mu = k_2^\mu$ and $p_1^\mu - q^\mu = k_1^\mu$ and using $q^2 = -2MT$, we obtained $p_2 \cdot q$ and $p_1 \cdot q$ given in Eq. (3).

One can also use the explicit forms of p_1^μ , p_2^μ and q^μ in Eqs. (2a)-(2c) to compute these scalar products directly, e.g.,

$$p_1 \cdot q = E_\nu T - E_\nu \sqrt{(M + T)^2 - M^2} \cos \theta. \quad (4)$$

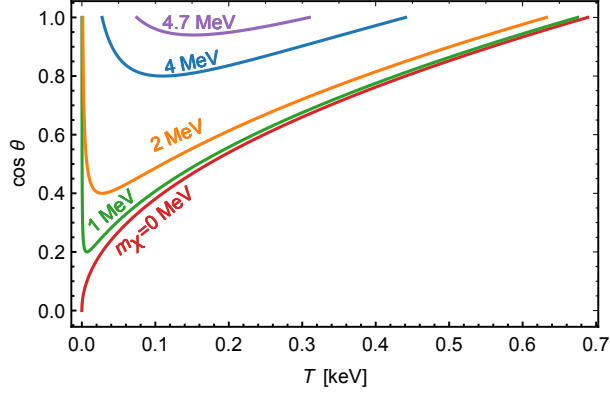


FIG. 2. Relation between $\cos\theta$ and T . This figure is produced according to Eq. (5) with $M = 72.6$ GeV (i.e. a Germanium detector) and $E_\nu = 5$ MeV. The case $m_\chi = 0$ has the same kinematics as the standard coherent elastic neutrino-nucleon scattering.

We can compare this result with Eq. (3) and obtain

$$\cos\theta = \frac{E_\nu T + MT + m_\chi^2/2}{E_\nu \sqrt{(M+T)^2 - M^2}}, \quad (5)$$

which reveals the relation between θ and T . In Fig. 2 we plot the relation for some specific values of m_χ in order to illustrate how $\cos\theta$ varies with T . Typically (for nonzero m_χ) $\cos\theta$ as a function of T has a minimum corresponding to the maximal scattering angle θ_{\max} .

By solving $d\cos\theta/dT = 0$ we obtain

$$\cos\theta_{\max} = \frac{m_\chi \sqrt{4M(E_\nu + M) - m_\chi^2}}{2ME_\nu}, \quad T_{\theta_{\max}} = \frac{Mm_\chi^2}{2ME_\nu - m_\chi^2 + 2M^2}. \quad (6)$$

For $T > T_{\theta_{\max}}$ ($T < T_{\theta_{\max}}$), $\cos\theta$ increases (decreases) with T . Therefore, $\cos\theta$ should be in the range

$$\cos\theta_{\max} \leq \cos\theta \leq 1, \quad (7)$$

and due to the upper bound, T can reach values in the range

$$T_{\min} \leq T \leq T_{\max}, \quad (8)$$

where T_{\min} and T_{\max} are determined by setting the left-hand side of Eq. (5) to 1 and solving the equation with respect to T . The solutions are

$$T_{\min/\max} = \frac{2ME_\nu^2 - m_\chi^2(E_\nu + M) \mp E_\nu \sqrt{4M^2E_\nu^2 - 4Mm_\chi^2(E_\nu + M) + m_\chi^4}}{2M(2E_\nu + M)}. \quad (9)$$

One can check that Eq. (9) has the following massless limit

$$\lim_{m_\chi \rightarrow 0} (T_{\min}, T_{\max}) = \left(0, \frac{2E_\nu^2}{M + 2E_\nu}\right), \quad (10)$$

which is consistent with the standard results of coherent elastic neutrino scattering.

Another important quantity is the minimal neutrino energy E_ν^{\min} necessary to create a massive particle χ :

$$E_\nu^{\min} = m_\chi + \frac{m_\chi^2}{2M}, \quad (11)$$

which is obtained by solving $T_{\min} = T_{\max}$. If E_ν is lower than E_ν^{\min} , χ cannot be produced in the scattering. In the limit when χ can just be produced, we have

$$\lim_{E_\nu \rightarrow E_\nu^{\min}} T_{\min} = \lim_{E_\nu \rightarrow E_\nu^{\min}} T_{\max} = \frac{m_\chi^2}{2(M + m_\chi)}. \quad (12)$$

An interesting difference between the cases of massive and massless χ occurs at T_{\min} . From Eq. (5) one can obtain

$$T \rightarrow T_{\min} \implies \cos \theta \rightarrow \begin{cases} 1, & \text{for } m_\chi \neq 0, \\ 0, & \text{for } m_\chi = 0, \end{cases} \quad (13)$$

which implies that in the minimal recoil limit for massive χ the nucleus after scattering moves along the same direction as the incoming neutrino ($\theta = 0$), while for massless χ it moves in the perpendicular direction ($\theta = 90^\circ$).

We would like to clarify here that we are discussing T approaching T_{\min} instead of being exactly equal to T_{\min} , because for $m_\chi = 0$, according to Eq. (10), T_{\min} is exactly zero. If $T = T_{\min} = 0$, strictly speaking, $\cos \theta$ is not well defined because it implies that the nucleus after scattering stays at rest. If T is approaching T_{\min} but remains nonzero, then $\cos \theta$ indeed is very close to zero for $m_\chi = 0$. For T fixed at a very small but nonzero value, when m_χ increases from zero to nonzero values, $\cos \theta$ will rise steeply (depending on the smallness of T) to 1 — as shown in Fig. 2. Therefore there is no inconsistency in the minimal recoil limit of $m_\chi = 0$ and $m_\chi \neq 0$. Although the T - $\cos \theta$ relation in the minimal recoil limit is very sensitive to small m_χ , experimentally it is difficult to observe this behavior due to rather small recoil energies.

B. Cross sections

The exchanged scalar S is generally assumed to be massive with its mass denoted by m_S . We evaluate the cross section without assuming $m_S^2 \ll q^2$ or $m_S^2 \gg q^2$. The heavy/light mass limits will be discussed below.

From the Feynman diagram in Fig. 1 and the relevant Lagrangian (1), one can straightforwardly write down the scattering amplitudes for (anti)neutrino initial state

$$i\mathcal{M}(\nu N \rightarrow \chi N) = \bar{u}^{s'}(k_1) (iy_\chi) P_L u^s(p_1) \frac{-i}{q^2 - m^2} \bar{u}^{r'}(k_2) (iy_N) u^r(p_2), \quad (14)$$

$$i\mathcal{M}(\bar{\nu} N \rightarrow \bar{\chi} N) = \bar{v}^s(p_1) P_R (iy_\chi) v^{s'}(k_1) \frac{-i}{q^2 - m^2} \bar{u}^{r'}(k_2) (iy_N) u^r(p_2), \quad (15)$$

where spinor superscripts denote spin and we have inserted the left-/right-handed projectors $P_L \equiv (1 - \gamma^5)/2$ and $P_R \equiv (1 + \gamma^5)/2$ since the neutrino sources can only emit left-handed neutrinos or right-handed antineutrinos. Using FeynCalc [33, 34] we compute $|i\mathcal{M}|^2$ for both cases. The result is identical for both neutrino and antineutrino scattering, namely

$$|i\mathcal{M}|^2 = \frac{8E_\nu^2 M^2 y^4}{(2MT + m_S^2)^2} K, \quad (16)$$

with the combined coupling constant

$$y^4 = y_\chi^2 y_N^2. \quad (17)$$

The dimensionless quantity K is typically $\mathcal{O}(1)$ and reads

$$K = \left(1 + \frac{T}{2M}\right) \left(\frac{MT}{E_\nu^2} + \frac{m_\chi^2}{2E_\nu^2}\right). \quad (18)$$

We will in what follows set limits using experiments with different nuclear targets. To reduce the dependence of the limits on the type of the nucleus we define

$$\bar{y} \equiv \frac{y}{\sqrt{A}}, \quad (19)$$

where A is the nucleon number (sum of neutron and proton numbers). Since \sqrt{A} has been factored out, \bar{y} has little dependence on the type of nuclei. For example, for Ge and CsI detectors we obtain¹

$$\bar{y} \approx \begin{cases} \sqrt{|(0.56y_n + 0.44y_p)y_\chi|} & \text{(for Ge target),} \\ \sqrt{|(0.58y_n + 0.42y_p)y_\chi|} & \text{(for CsI target),} \end{cases} \quad (20)$$

where the Yukawa couplings of the scalar S to neutrons and protons are denoted with y_n and y_p respectively. Clearly, \bar{y} for Ge (employed at the CONUS experiment) is approximately the same as \bar{y} for CsI (currently employed at the COHERENT experiment).

The differential cross section, according to Eq. (16), reads

$$\frac{d\sigma}{dT} = \frac{|i\mathcal{M}|^2}{32\pi M E_\nu^2} = \frac{M\bar{y}^4}{4\pi A^2 (2MT + m_S^2)^2} K. \quad (21)$$

One can straightforwardly check that in the limit $m_\chi^2 \rightarrow 0$ the result in Eq. (21) is consistent with the standard cross section of elastic neutrino scattering [1].

C. Signals and constraints

Now let us study the signal of our new fermion χ in $\text{CE}\nu\text{NS}$ experiments. We will focus on two experiments, namely COHERENT [1] and CONUS [20]. For the former, we will present the limits on the relevant parameters in $\nu N \rightarrow \chi N$ scattering based on the recent data release, whereas for the latter experiment we obtain sensitivities.

The COHERENT experiment is based on neutrino emission from the Spallation Neutron Source at Oak Ridge National Laboratory. A crystal scintillator detector with 14.6 kg CsI was used in its recent measurement of $\text{CE}\nu\text{NS}$ and the SM signal has been observed with 6.7σ confidence. The neutrinos are produced via π^+ decay ($\pi^+ \rightarrow \mu^+ + \nu_\mu$) and subsequently μ^+ decay ($\mu^+ \rightarrow e^+ + \bar{\nu}_\mu + \nu_e$). In this experiment, both π^+ and μ^+ approximately decay at rest, which allows us to obtain the analytical expressions for neutrino spectra [35]

$$\phi_{\nu_\mu}(E_\nu) = \phi_0 \delta(E_\nu - E_{\nu 0}), \quad \text{with } E_{\nu 0} = \frac{m_\pi^2 - m_\mu^2}{2m_\pi} \approx 29.8 \text{ MeV}, \quad (22)$$

¹ See Sec. II.C of Ref. [14], where the conversion from y_n and y_p to more fundamental quark Yukawa couplings is discussed.

$$\phi_{\bar{\nu}_\mu}(E_\nu) = \phi_0 \frac{64E_\nu^2}{m_\mu^3} \left(\frac{3}{4} - \frac{E_\nu}{m_\mu} \right), \quad (E_\nu < m_\mu/2), \quad (23)$$

$$\phi_{\nu_e}(E_\nu) = \phi_0 \frac{192E_\nu^2}{m_\mu^3} \left(\frac{1}{2} - \frac{E_\nu}{m_\mu} \right), \quad (E_\nu < m_\mu/2), \quad (24)$$

which contains a monochromatic component ϕ_{ν_μ} (i.e. all ν_μ have the same energy $E_{\nu 0}$).

The CONUS experiment measures CE ν NS of reactor neutrinos ($\bar{\nu}_e$) from a 3.9 GW nuclear power plant in Brokdorf, Germany. The detector is a Germanium semiconductor containing 4 kg of natural Ge ($A = 72.6$ in average), which is set at a distance of 17 meters from the reactor. To compute the event rates we adopt the reactor neutrino flux computed in [36, 37] and normalize the total flux to $2.5 \times 10^{13} \text{ s}^{-1} \text{ cm}^{-2}$. CONUS data taking has started in April 2018 and recently a preliminary 2.4σ statistical significance for observing the process was announced [20].

The event numbers in both experiments can be computed in the following way: in the i -th recoil energy bin ($T_i < T < T_i + \Delta T$), the total event number² N_i consists of the SM contribution N_i^{SM} and the new physics contribution N_i^{new} , i.e.

$$N_i = N_i^{\text{SM}} + N_i^{\text{new}}, \quad (25)$$

which are computed by

$$N_i^{\text{SM}} = \Delta t N_{\text{nucleus}} \int_{T_i}^{T_i + \Delta T} dT \int dE_\nu \phi(E_\nu) \times \frac{d\sigma^{\text{SM}}}{dT}(T, E_\nu) \times \Theta^{\text{SM}}(T, E_\nu), \quad (26)$$

$$N_i^{\text{new}} = \Delta t N_{\text{nucleus}} \int_{T_i}^{T_i + \Delta T} dT \int dE_\nu \phi(E_\nu) \times \frac{d\sigma^{\text{new}}}{dT}(T, E_\nu) \times \Theta^{\text{new}}(T, E_\nu), \quad (27)$$

where

$$\Theta^{\text{SM}}(T, E_\nu) \equiv \begin{cases} 1 & 0 < T < T_{\text{max}}^{\text{SM}}(E_\nu), \\ 0 & \text{otherwise,} \end{cases}$$

$$\Theta^{\text{new}}(T, E_\nu) \equiv \begin{cases} 1 & T_{\text{min}}(E_\nu) < T < T_{\text{max}}(E_\nu), \\ 0 & \text{otherwise.} \end{cases} \quad (28)$$

Here ϕ is the neutrino spectrum, N_{nucleus} is the number of nuclei in the detector and t is the data taking period. The explicit expressions of $T_{\text{max}}^{\text{SM}}$, T_{min} and T_{max} are given in Eqs. (9) and (10). We note that we have included a form factor $F(q^2)$ in the cross section for the COHERENT experiment, where we take the parametrization given in Ref. [38], see Fig. 1(a) therein. For the CsI detectors used in COHERENT, since the atomic number of Xe (54) is between Cs (55) and I (53), it is a good approximation to use the Xe form factor for both Cs and I. For reactor neutrinos, we can set $F(q^2) = 1$ due to the low recoil energy.

Using the above equations, we can compute the event numbers and study the signal of new physics in these two experiments. In Fig. 3, we present the event distributions for several choices of (\bar{y}, m_χ, m_S) parameters together with the ratio of N_i/N_i^{SM} for both CONUS (left) and COHERENT (right). We selectively choose several values for m_χ (0 MeV and 3 MeV for CONUS; 3 MeV and 30 MeV for COHERENT) to illustrate the effect of m_χ on CE ν NS. Light and heavy

² In COHERENT experiment there are 3 neutrino species (see Eqs. (22) to (24)). In that case the total event rate is obtained by summing individual contributions from the three species.

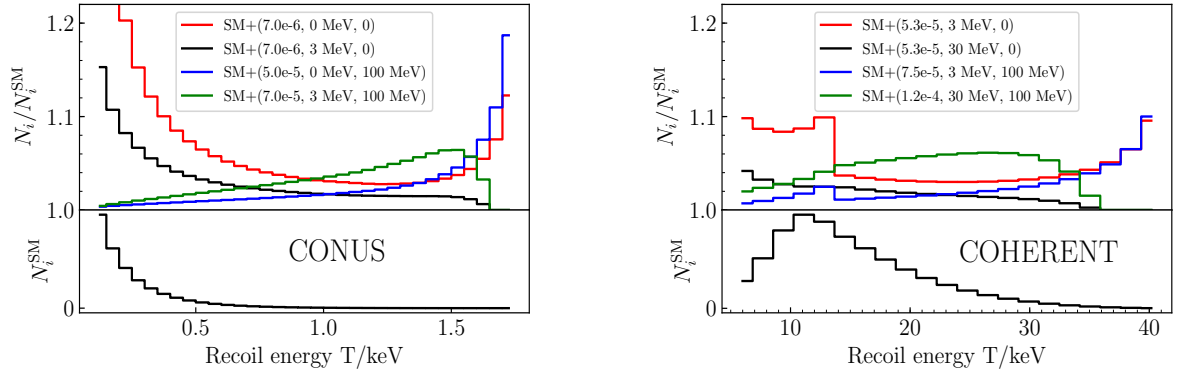


FIG. 3. Event distributions and spectrum distortions due to the new channel ($\nu N \rightarrow \chi N$) in CONUS (left) and COHERENT (right). N_i^{SM} and N_i are the event numbers for SM-only and SM plus new physics, respectively. In the upper panels the ratio of the total and SM-only event rate is shown with the corresponding (\bar{y}, m_χ, m_S) indicated in the parentheses. In the lower panels we indicate the recoil spectrum of the SM process in arbitrary units.

mediator cases have been illustrated by considering both $m_S = 0$ MeV and $m_S = 100$ MeV. The kinks of the red and blue curves appearing in the right panel at $T \approx 14$ keV are caused by the monochromatic $\phi_{\nu\mu}$ in COHERENT. The green and black curves correspond to $m_\chi = 30$ MeV. Since the monochromatic ν_μ neutrinos of 29.8 MeV energy do not have sufficient energy to produce χ there are no similar kinks in these two curves.

By comparing N_i with the observed event numbers we can obtain the constraints on the χ coupling to neutrinos and nuclei. For COHERENT, the observed event numbers have been published in Ref. [1] which can be used directly in our data fitting procedure. The recoil threshold in COHERENT is controlled by the signal acceptance fraction (see Fig. S9 of Ref. [1]) which drops down quickly when the number of photoelectrons n_{PE} ($n_{\text{PE}} \approx 1.17 T/\text{keV}$) is less than 20, and approximately vanishes when $n_{\text{PE}} < 5$. Therefore, in fitting the COHERENT data we import the signal acceptance fraction directly instead of setting a distinct threshold. The systematic and statistical uncertainties have been combined and provided in Fig. 3 of Ref. [1], and are employed directly in our data fitting.

The CONUS data has not been published, and hence we assume that their findings will be compatible with the SM prediction after 1 year of data taking with a 4 kg detector (thus 1 year \times 4 kg exposure). This allows us to compute sensitivity of CONUS on the production of χ . More explicitly, we adopt the following χ^2 -function comparing N_i with N_i^{SM} :

$$\chi^2 = \sum_i \frac{[(1+a)N_i - N_i^{\text{SM}}]^2}{\sigma_{\text{stat},i}^2 + \sigma_{\text{sys},i}^2} + \frac{a^2}{\sigma_a^2}, \quad (29)$$

$$\sigma_{\text{stat},i} = \sqrt{N_i + N_{\text{bkg},i}}, \quad \sigma_{\text{sys},i} = \sigma_f(N_i + N_{\text{bkg},i}). \quad (30)$$

Here $1+a$ is a rescaling factor with an uncertainty $\sigma_a = 2\%$ which mainly comes from the overall uncertainty of the neutrino flux. In addition, other systematic uncertainties may change the shape of the event spectrum, which is parametrized by σ_f and assumed to be 1%. The flux uncertainties used here are somewhat optimistic. According to the previous theoretical calculations [36, 37, 39], the flux uncertainty at 5 MeV is about 3%. In the next few years, both the theoretical

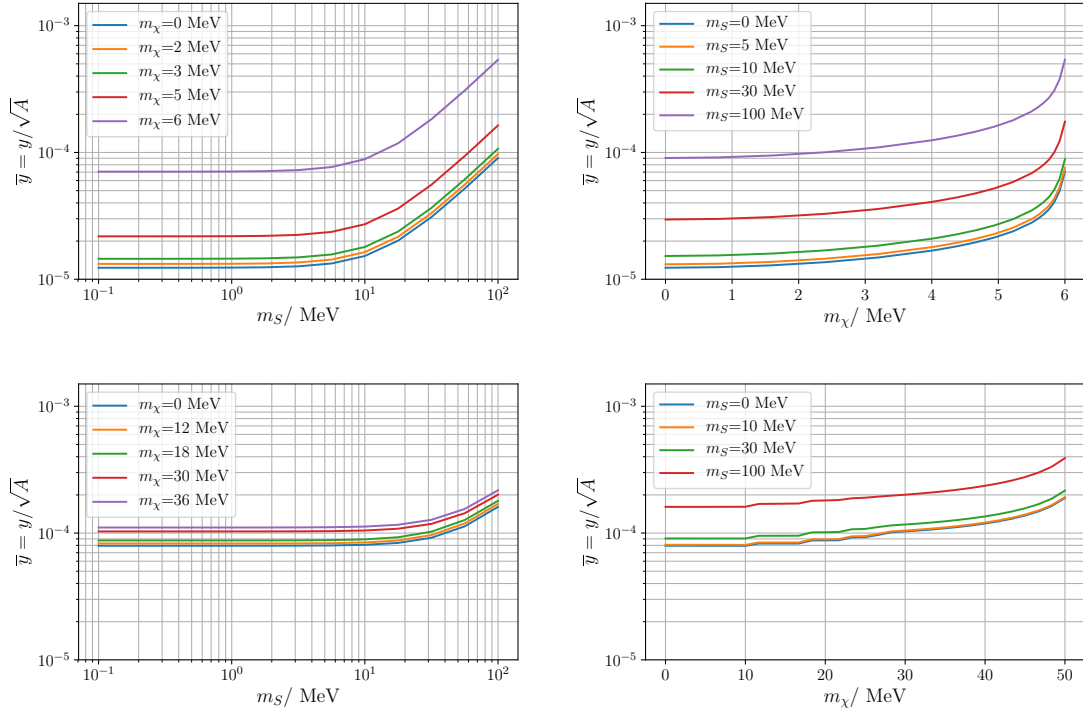


FIG. 4. Constraints (with 90% C.L.) of CONUS (upper panels) and COHERENT (lower panels) in $\bar{y} - m_S$ (left panels) and $\bar{y} - m_\chi$ (right panels) parameter space.

understanding and experimental measurements will be considerably improved [40–42] so that the flux will be determined more precisely. The background $N_{\text{bkg}, i}$ in each bin is 1 count/(day·keV·kg). For the nucleus recoil threshold we take 1.2 keV.

The results are presented in Fig. 4 where we show the constraints in the $\bar{y} - m_S$ plane (with m_χ fixed) and the $\bar{y} - m_\chi$ plane (with m_S fixed). In the $\bar{y} - m_S$ panels, the bounds are almost flat when $m_S < 2$ MeV (CONUS) or $m_S < 10$ MeV (COHERENT), which can be understood from Eq. (21) where, for small m_S , $2MT$ dominates over m_S^2 in the denominator. Similarly, in the $\bar{y} - m_\chi$ plots, the bounds are also approximately flat for small m_χ which can be understood from the K factor in Eq. (18). However, the large mass behaviors are different for m_χ and m_S . As shown in the left panels of Fig. 4, the curves are approximately linear for large m_S because in this case the cross section is proportional to $(\bar{y}/m_S)^4$. On the other hand, large m_χ can only be constrained by the events with high E_ν . If m_χ is larger than the maximal value of E_ν of the neutrino flux, then there will be no constraint at all because neutrinos do not have sufficient energy to produce χ . For reactor neutrinos, the event rate above 6 MeV is essentially too low to have a significant impact and hence the sensitivity to the new physics scenario diminishes. Therefore, the CONUS curves in the right panel rise up quickly around 6 MeV. For COHERENT, the maximal E_ν is about 53 MeV (half of m_μ) but, unlike in CONUS, the flux is not suppressed when E_ν is approaching 53 MeV, so the curves do not rise so quickly when m_χ is close to the maximal E_ν .

In the future, the measurement of CE ν NS will be significantly improved by lower thresholds, larger fiducial masses, and longer exposure times, etc. For reactor neutrinos, lower thresholds can increase the statistics drastically because the current threshold actually only allows CONUS to measure the high energy tail of the reactor neutrino flux. For COHERENT, using lower threshold detectors will not improve the measurement significantly. This is because, unlike reactor neutrinos,

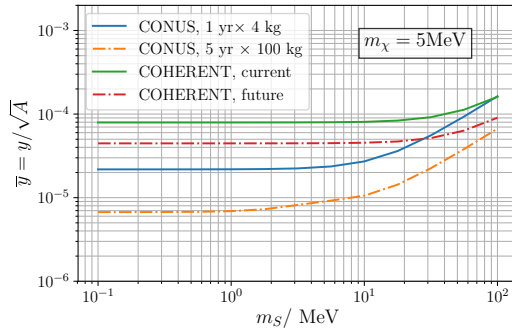


FIG. 5. Future sensitivities of CONUS (5 yr \times 100 kg exposure, 0.1 keV threshold) and COHERENT (statistics \times 100) on the benchmark $m_\chi = 5$ MeV. For more details about the future configurations, see the text.

the majority of the neutrinos produced by μ^+ or π^+ decays are not in the low-energy region—see Fig. 3 for comparison. Consequently, lower thresholds for COHERENT cannot enhance the event numbers considerably and thus cannot improve the sensitivity significantly. We will consider here the following two benchmark configurations to illustrate the future sensitivities of CE ν NS experiments. The first one is running CONUS for 5 years with 100 kg Ge, and a considerably improved threshold down to 0.1 keV. In addition, the theoretical uncertainties of reactor neutrino flux are assumed to be reduced by a factor of 2. The second is (instead of doing a very detailed study of various other detectors and target materials that are planned [43]) increasing the statistics of COHERENT by a factor of 100, which could be achieved by, e.g., a 20 times larger fiducial mass with 5 times longer exposure. The systematic uncertainties are correspondingly reduced so that we assume the overall uncertainty is reduced by a factor of $\sqrt{100} = 10$. In Fig. 5, we show the sensitivities of these two future experiments together with their current constraints/sensitivities. Here, m_χ is set at 5 MeV as a benchmark value.

Let us now discuss other limits on the scenario under study. Regarding CE ν NS, aspects of light scalars coupling to neutrinos and nuclei were explored in Ref. [14]. Since in our framework a massive MeV-scale fermion χ is involved, most limits are expected to be weaker than the ones collected in Ref. [14], where only couplings to nuclei and light neutrinos were considered. It is in addition more complicated to obtain precise limits, so we focus here on giving reasonably robust estimates. It was found in Ref. [14] that all limits from terrestrial experiments, e.g. n -Pb scattering and meson decay experiments, are weaker than the bound from COHERENT as well as the CONUS sensitivity. BBN constraints, however, are relevant for $\mathcal{O}(1)$ MeV-scale S , and thus the $m_S = 0$ curves in Fig. 4 should be interpreted as an illustration to show the strength of the limit in the small mass regime. When considering the χ density evolution in the early Universe (see Section IV), we will actually take $m_S \approx 10 - 100$ MeV.

We should also mention limits from Supernova 1987A. If efficiently produced, the light states can carry a significant amount of energy from the Supernova core. In such case, the amount of energy carried by active neutrinos would be too small to match the observation of Supernova 1987A and hence a limit can be set. The leading process for the production of S is $\nu\nu \rightarrow SS$ via t -channel χ exchange and it is suppressed by the fourth power of the small coupling y_χ . As χ is concerned, in Ref. [44] the authors presented, within a specific model, that the cross section for scattering of a new light fermion on protons and electrons is constrained by Supernova 1987A cooling arguments to values comparable to the corresponding cross sections for neutrinos. This can be understood as follows: if a novel fermion acts as a fourth neutrino species inside of the star, it will carry away

energy comparable to the one carried away by the individual active neutrino species. This suggests that $\sim 25\%$ of the energy budget would be carried away by χ . Given the astrophysical uncertainties associated to Supernova 1987A, exotic particles can carry away up to 50% of the total energy of the collapse [45, 46]. This corresponds again roughly to a new cross section of similar magnitude as the SM one. The reachable parameter values from Fig. 4 fulfill this constraint. Hence, we infer that the cooling arguments are not excluding the relevant parameter space. Finally, note that χ , being an MeV-scale particle, can not be resonantly produced through an MSW effect [47–49]. Such effect is very relevant for keV-scale particles for which strong limits can be derived [50].

III. χ AND NEUTRINO MASS GENERATION

In this section we will discuss the possible connection of the new fermion χ to neutrino mass generation. Any fermion that couples to light active neutrinos must be investigated with regard to its contribution to neutrino mass.

Let us first discuss the nature of the scalar S that appears in our framework. Given our preference for light S , such construction is not achievable with representations higher than singlets. Namely, S can obviously not be the SM Higgs due to its tiny couplings with u and d quark as well as its heavy mass which would further suppress the strength of the $CE\nu NS$ process. If we replace the SM Higgs by a novel Higgs doublet Φ with possibly larger couplings to quarks (and hence nuclei), we face the problem of a necessary huge mass splitting between the light neutral component and the charged ones, which have not been seen. An option would be to consider the following gauge invariant 5-dimensional operator in the effective theory formalism

$$\mathcal{L} \supset \frac{1}{\Lambda} (S\bar{\chi}) (\tilde{H}^\dagger L) + \text{h.c.}, \quad (31)$$

with singlets S and χ , where Λ represents the scale of new physics. After electroweak symmetry breaking this operator yields an interaction term

$$\frac{v}{\Lambda} S\bar{\chi}\nu. \quad (32)$$

By assuming furthermore non-vanishing interactions between S and nuclei (or light quarks), the $CE\nu NS$ occurs through the process shown in Fig. 1. We will now discuss a minimal model containing SM singlets only, which will generate the effective Lagrangian in Eq. (31).

A. The Model

We supplement the SM particle content with

$$\chi \sim (1, 1, 0), \quad N_R \sim (1, 1, 0), \quad S \sim (1, 1, 0), \quad (33)$$

where χ and N_R are Majorana fermions and S is a real scalar. The quantum numbers under the SM gauge group $SU(3)_c \times SU(2)_L \times U(1)_Y$ are indicated in brackets, and clearly no charged degrees of freedom are introduced. One of the goals of this section is to demonstrate that the neutrino masses can be generated from this extended fermion sector via a modified type-I seesaw mechanism [51–54]. This means that we would require at least two generations of novel fermions which participate in this mechanism, such that at most one light neutrino is massless. Still, for simplicity, throughout this section we will focus on the 1-generation case which can be straightforwardly extended. Similarly,

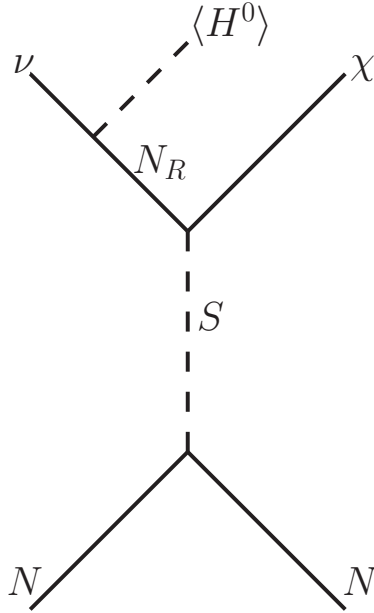


FIG. 6. The process for $CE\nu NS$ in the UV complete realization given in Section III A.

we will also restrict our discussion to one active neutrino flavor state, namely for definiteness the electron (anti)neutrino $\bar{\nu}_e$.

The relevant part of the Lagrangian reads

$$\mathcal{L} \supset y_1 \bar{N}_R \tilde{H}^\dagger L + \frac{1}{2} M_N \bar{N}_R N_R^c + y_2 \bar{\chi} \tilde{H}^\dagger L + \frac{1}{2} m_\chi \bar{\chi} \chi^c + y_3 \bar{\chi} S N_R^c + M_1 \bar{N}_R \chi^c + \text{h.c.}, \quad (34)$$

where y_i ($i = 1, 2, 3$) are the Yukawa couplings³, m_χ and M_N are Majorana masses of χ and N_R fields, respectively, and M_1 is the Dirac mass which is allowed by gauge symmetries.

This Lagrangian is a minimal UV complete realization of Eqs. (31) and (32) with fermion singlet N_R interacting with the fields given in both brackets of Eq. (31) through Yukawa couplings y_1 and y_3 (see Eq. (34)). We will show that the allowed values of M_N exceed the characteristic momentum exchange q^2 in $CE\nu NS$ experiments, which justifies the analysis setup in Section II. If $M_N^2 \gg q^2$, we can easily relate the parameters of the full theory with Λ and obtain $\Lambda = M_N/(y_1 y_3)$. If that was not the case, the topology shown in Fig. 6 including N_R as the dynamical degree of freedom should be considered.

More importantly, within the presented model, we will demonstrate the existence of parameter space that can be probed by $CE\nu NS$ experiments, generates neutrino masses in the right ballpark, and is not excluded from the new physics searches at neutrino oscillation facilities, beam dump experiments, colliders, etc. This indicates the importance of the $CE\nu NS$ in future new physics searches as there are scenarios where it could yield the strongest limits or perhaps even lead to new discoveries.

After electroweak symmetry breaking, the neutral fermion mass matrix reads

$$(\bar{\nu}_L^c \quad \bar{\chi} \quad \bar{N}_R) \begin{pmatrix} 0 & y_2 v & y_1 v \\ y_2 v & m_\chi & M_1 \\ y_1 v & M_1 & M_N \end{pmatrix} \begin{pmatrix} \nu_L \\ \chi^c \\ N_R^c \end{pmatrix}, \quad (35)$$

³ In this work we do not study CP violation in the lepton sector so these couplings can be taken real for simplicity.

where $v \equiv \langle H^0 \rangle = 174$ GeV and we assumed that S does not develop a non-vanishing vacuum expectation value.

We furthermore assume for the mass matrix given in Eq. (35) that $M_1 \ll M_N$. In this way, the mixing between χ and N_R is suppressed and hence, the masses of heavy new fermions essentially match the parameters in the flavor basis, m_χ and M_N . Contrary, if $M_1 \simeq M_N$, the two physical masses would be of similar size which is not wanted in our scenario.

We start by performing a rotation in the 1-2 plane by an angle $\theta_{e\chi} = y_2 v/m_\chi \ll 1$. As discussed above, m_χ is the physical mass of a particle produced in CE ν NS experiments. We take $m_\chi = 5$ MeV as an illustrative number. The bounds on the mixing of active neutrinos with heavy fermions have been extensively studied in the literature. From Refs. [55–57] we infer that the constraint on the mixing between ν_e and χ for $m_\chi = 5$ MeV reads⁴

$$\theta_{e\chi}^2 \leq 10^{-7} \quad \implies \quad y_2 \lesssim 9 \times 10^{-9}, \quad (36)$$

and is set by neutrinoless double beta decay experiments. Weaker limits apply for the other flavors, which therefore can be accommodated more easily. The mass matrix after the 1-2 rotation reads approximately

$$\mathcal{M} = \begin{pmatrix} -y_2^2 v^2/m_\chi & 0 & y_1 v \\ 0 & m_\chi & y_1 y_2 v^2/m_\chi \\ y_1 v & y_1 y_2 v^2/m_\chi & M_N \end{pmatrix}, \quad (37)$$

from where one can infer that χ may serve as a potential source of neutrino mass. By taking the upper value of y_2 in Eq. (36) we obtain $m_\nu \approx y_2^2 v^2/m_\chi \sim 0.1$ eV which matches the required order of magnitude for neutrino mass.

It was demonstrated in Section II that the numerical analysis of CE ν NS for $m_S \lesssim 100$ MeV yields the limit

$$\bar{y} \equiv \sqrt{\frac{y_N}{A} y_\chi} = \sqrt{\frac{y_N}{A} \frac{v}{M_N} y_1 y_3} \lesssim [10^{-5}, 10^{-4}], \quad (38)$$

where y_χ was introduced in Eq. (1) and y_N/A roughly corresponds to the coupling strength to individual quarks. The values indicated in square brackets represent the range in which the bound, depending on specific values of m_S and m_χ , is set (see Fig. 4). We assume $y_N/A \simeq y_\chi$, i.e. similar size of the S coupling to quarks and fermions, such that

$$y_\chi \equiv \frac{v}{M_N} y_1 y_3 \lesssim [10^{-5}, 10^{-4}] \quad (39)$$

approximately holds. Having now a feeling for the numbers in Eq. (37), we continue the diagonalization. Performing a rotation in the 1-3 plane by an angle $\theta_{eN} = y_1 v/M_N \ll 1$ and using this expression as well as Eq. (39) we can relate the mixing angle with the upper limit from CE ν NS experiments

$$\theta_{eN} \simeq \frac{[10^{-5}, 10^{-4}]}{y_3}. \quad (40)$$

Clearly, y_3 must not be tiny as otherwise the large mixing would pose a problem for $M_N \lesssim \mathcal{O}(\text{TeV})$. We can safely assume $y_3 = \mathcal{O}(1)$ because it parametrizes the strength of the interaction between

⁴ Somewhat stronger cosmological limits exist in the literature [58]. Unlike laboratory limits, these can be evaded by assuming for instance a novel decay channel for χ .

three hidden particles and moreover S does not mix with the SM Higgs. By inserting $v = 174$ GeV in Eq. (39) we obtain the relation

$$M_N \simeq y_1 [10^6, 10^7] \text{ GeV}. \quad (41)$$

The seesaw contribution to the neutrino mass from mixing between ν_e and N_R is then

$$m_\nu \sim \frac{y_1^2 v^2}{M_N} \simeq y_1 [10^{-3}, 10^{-2}] \text{ GeV}, \quad (42)$$

which gives the upper bound on y_1 from neutrino mass considerations

$$y_1 \lesssim [10^{-8}, 10^{-7}]. \quad (43)$$

From Eqs. (41) and (43) we infer that the M_N values which can contribute to this neutrino mass generation are in the $\mathcal{O}(10^{-2} - 1)$ GeV mass range. Finally, we need to check if the mixing given in Eq. (40) is compatible with such masses. To this end, we again employ the limits from Refs. [55–57] and infer that $M_N = \mathcal{O}(1)$ GeV is fully consistent, whereas the smaller values are marginally allowed, i.e. in tension with the constraints from neutrinoless double beta decay experiments, big bang nucleosynthesis as well as the PS191 [59] beam dump experiment. Interestingly, GeV-scale M_N will be testable at some upcoming experiments such as DUNE [60], SHiP [61], FASER [62–64], NA62 [65] and MATHUSLA [66].

In summary, parameters that are compatible with all available laboratory constraints and give an observable signal in coherent scattering experiments, give a neutrino mass of order

$$\left(\frac{m_\nu}{0.1 \text{ eV}}\right) \approx (1-x) \left(\frac{y_1}{10^{-7.25}}\right)^2 \left(\frac{\text{GeV}}{M_N}\right) + x \left(\frac{y_2}{10^{-8.75}}\right)^2 \left(\frac{\text{MeV}}{m_\chi}\right), \quad (44)$$

which is compatible with observation. Here, $x \in [0, 1]$ denotes relative contribution to the active neutrino mass from χ and N_R .

IV. χ AS DARK MATTER PARTICLE

Limits on m_S from terrestrial experiments as well as astrophysics were discussed in Section II. This section is devoted to the evaluation of the cosmic abundance of χ . As a first observation, we note that the smallness of m_χ relative to the electroweak scale implies that the production of DM from freeze-out might not yield desired results and signifies the preference for non-thermal production. Note further that within our framework there is no possibility for χ to decay into a pair of electrons or neutrinos. However, there could be tree-level ($\chi \rightarrow 3\nu$) and radiative decays ($\chi \rightarrow \nu\gamma$). From the expressions for the decay rates of these processes [50, 67] we infer that in order to ensure χ stability, $\theta_{e\chi} \lesssim 4.8 \cdot 10^{-9}$ for $m_\chi = 5$ MeV. The implied tiny value of y_2 does not jeopardize our new physics scenario at CE ν NS experiments because the rate for $\nu N \rightarrow \chi N$ depends on y_1 and y_3 couplings, but not on y_2 . Note however from Eq. (44) that neutrino mass will be dominated by M_N in this case.

If χ is the DM particle, CE ν NS experiments would yield an entirely novel method for searching (MeV-scale) DM. Note that dark matter in CE ν NS experiments was discussed already in [68, 69], where kinetically mixed dark photons decay into DM pairs which subsequently scatters at CE ν NS experiments (note that the neutrino sources of those experiments also generate photons). Here, we will propose a novel framework by demonstrating that the DM particle can be produced directly via CE ν NS and the effects of such process are imprinted in the measurable recoils of the nuclei.

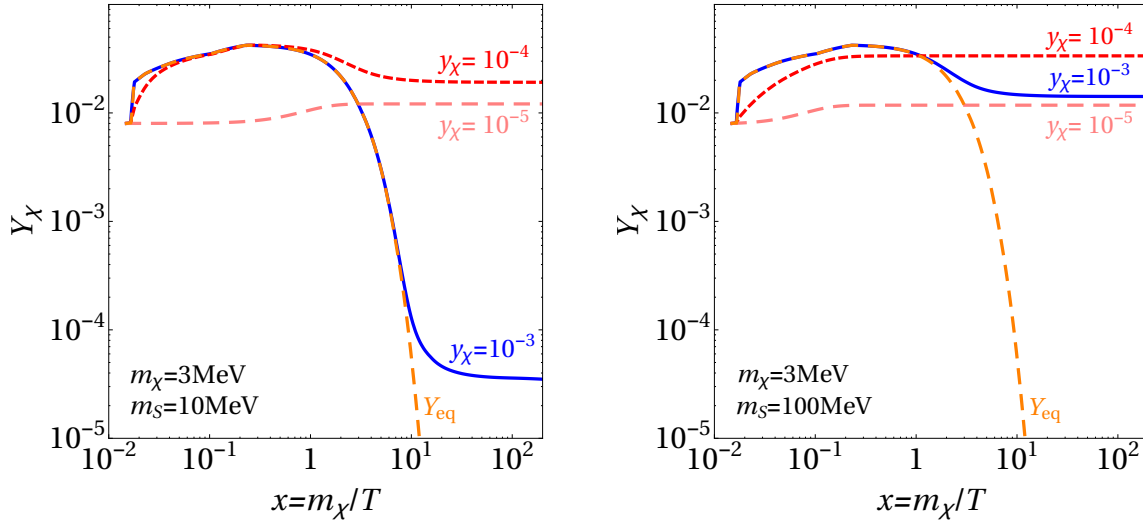


FIG. 7. In left (right) panel we show the evolution of Y_χ for several different values of y_χ with fixed $m_\chi = 3$ MeV and $m_S = 10$ MeV ($m_S = 100$ MeV). For larger couplings, characteristic freeze-out curves are easy to identify whereas χ is “frozen-in” for weaker $\chi\chi \leftrightarrow \bar{\nu}\nu$ interaction. In the latter scenario, the χ abundance is set primarily by the initial condition, i.e. not-vanishing Y_χ at T_{QCD} .

Interestingly, this would resemble DM search in direct detection experiments because in both cases the observable signal is the nuclear recoil. While nuclear recoil in direct detection experiments stems from DM-nucleus interaction, in $\text{CE}\nu\text{NS}$ such effect is caused by neutrinos. Thus, the main goal would be to distinguish between the SM coherent neutrino scattering events and “new physics” events in which χ is produced. We have shown in Section II that the distributions of the recoil energy corresponding to these two cases can be vastly different and it is possible to discriminate between them. These arguments strongly motivate the search for DM at $\text{CE}\nu\text{NS}$ experiments if χ can indeed play the role of DM. Hence, in what follows we will discuss if and how χ can be produced in right amounts. We rely on the UV complete model introduced in Section III which was already shown to be successful in generating non-vanishing neutrino masses.

In order to realize the $\text{CE}\nu\text{NS}$ process shown in Fig. 1 we require S to interact with quarks as well as with χ and neutrinos. The Lagrangian for these interactions reads

$$\mathcal{L} \supset y_{sq} S \bar{q} q + y_\chi S \bar{\chi} \nu, \quad (45)$$

where $y_{sq} \simeq y_N/A$ and y_χ are the couplings to quarks and leptons, respectively. We consider the case in which neither of these couplings is weaker than $\mathcal{O}(10^{-6})$. For an UV complete model from which Eq. (45) stems after electroweak symmetry breaking, we refer the reader to Sections II and III.

For $m_S \lesssim 100$ MeV and $y_{sq} \geq \mathcal{O}(10^{-6})$, the decay and inverse decay widths of the process $S \leftrightarrow \bar{q}q$ are much larger than the value of the Hubble parameter across the relevant temperatures. Thus, S is in thermal equilibrium with the SM bath. At the temperatures below the QCD phase transition ($T_{\text{QCD}} \simeq 200$ MeV) quarks are no longer relevant degrees of freedom. The vast majority of the formed mesons and baryons are non-relativistic and hence effectively disappear from the SM thermal bath shortly below T_{QCD} (the only exception are pions which are somewhat lighter). The $S \leftrightarrow \bar{q}q$ interaction which was keeping S in thermal equilibrium is not relevant below T_{QCD} . However, even below T_{QCD} , S can be in thermal equilibrium through the process $SS \leftrightarrow \bar{\nu}\nu$, provided there is a sufficiently large Yukawa coupling y_χ . Such process occurs via t -channel exchange of χ

and is governed exclusively by the second term in Eq. (45). Note that S should decay shortly below T_{QCD} into χ and neutrinos in order not to violate any of the BBN predictions. For the parameter values we will take below this is indeed the case. It is also worthwhile to mention that the N_R , introduced in Section III to UV-complete the model, decay well above T_{QCD} due to their large y_3 coupling. On the other hand, the stability of χ is ensured by assuming a small value of y_2 which sufficiently suppresses $\chi \rightarrow 3\nu$ and $\chi \rightarrow \nu\gamma$ decays.

Above T_{QCD} , χ is in thermal equilibrium with S and hence also with the SM bath, due to rapid $S \leftrightarrow \chi\nu$ processes. Whether χ remains in contact with the SM bath at lower temperatures (after S decays) depends on the strength of the $\bar{\chi}\chi \leftrightarrow \bar{\nu}\nu$ process which occurs via t -channel exchange of S (hence is proportional to y_χ^4).

In order to accurately determine the present-day abundance of χ we solve the following Boltzmann equations [70, 71]

$$\begin{aligned} \frac{dY_\chi}{dx} &= \frac{1}{3H} \frac{ds}{dx} \left[\langle\sigma v\rangle_{\bar{\chi}\chi \rightarrow \bar{\nu}\nu} (Y_\chi^2 - (Y_\chi^{\text{eq}})^2) - \frac{\Gamma_S}{s} \frac{K_1(\frac{m_S}{m_\chi} x)}{K_2(\frac{m_S}{m_\chi} x)} \left(Y_S - Y_\chi \frac{Y_S^{\text{eq}}}{Y_\chi^{\text{eq}}} \right) \right. \\ &\quad \left. + \langle\sigma v\rangle_{\bar{\chi}\chi \rightarrow SS} \left(Y_\chi^2 - Y_S^2 \left(\frac{Y_\chi^{\text{eq}}}{Y_S^{\text{eq}}} \right)^2 \right) \right], \\ \frac{dY_S}{dx} &= \frac{1}{3H} \frac{ds}{dx} \left[\langle\sigma v\rangle_{SS \rightarrow \bar{\nu}\nu} (Y_S^2 - (Y_S^{\text{eq}})^2) + \frac{\Gamma_S}{s} \frac{K_1(\frac{m_S}{m_\chi} x)}{K_2(\frac{m_S}{m_\chi} x)} \left(Y_S - Y_\chi \frac{Y_S^{\text{eq}}}{Y_\chi^{\text{eq}}} \right) \right. \\ &\quad \left. - \langle\sigma v\rangle_{\bar{\chi}\chi \rightarrow SS} \left(Y_\chi^2 - Y_S^2 \left(\frac{Y_\chi^{\text{eq}}}{Y_S^{\text{eq}}} \right)^2 \right) \right]. \end{aligned} \quad (46)$$

For a particle denoted with i we define the yield as $Y_i = n_i/s$ (superscript eq denotes equilibrium value), where n_i and s are number and entropy density, respectively. In addition, $x = m_\chi/T$, H is the Hubble parameter, $\langle\sigma v\rangle$ is the thermally averaged cross section for a given process (evaluated following Ref. [72]), $\Gamma_S = y_\chi^2 m_S/(8\pi)$, K_1 and K_2 are modified Bessel functions. The initial conditions are $Y_\chi(T_{\text{QCD}}) = Y_\chi^{\text{eq}}$ and $Y_S(T_{\text{QCD}}) = Y_S^{\text{eq}}$, since we argued above that the sizable coupling to free quarks leaves the particles in thermal equilibrium at temperatures above T_{QCD} .

The solution for $Y_\chi(x)$ is shown in Fig. 7. In both panels we set $m_\chi = 3$ MeV and show the results for $y_\chi = \{10^{-3}, 10^{-4}, 10^{-5}\}$ which are in the ballpark of testable values at CE ν NS experiments. In the (left) right panel, m_S is fixed to 10 MeV (100 MeV). Much smaller values of m_S are not considered due to the requirement $m_\chi < m_S$ which forbids χ to decay and is thus essential to render our DM candidate stable. We discuss and interpret the results from the figure in what follows.

In both panels we observe the standard thermal freeze-out of χ for $y_\chi = 10^{-3}$. The interaction which keeps χ in thermal equilibrium with the SM is $\bar{\chi}\chi \rightarrow \bar{\nu}\nu$, and the strength of this process increases by reducing m_S . Hence, for smaller m_S , the stronger interaction indicates that χ stays longer in the thermal equilibrium and undergoes freeze-out at later times (smaller temperatures) which implies smaller final abundance of χ . This is visible from Fig. 7 where the final value of Y_χ for $y_\chi = 10^{-3}$ (blue line) in the left panel (lighter S) is much smaller than the one shown in the right panel. By using the relation between the yield and the relic abundance

$$\Omega h^2 = 2.742 \cdot 10^5 \left(\frac{m_\chi}{1 \text{ MeV}} \right) Y_\chi, \quad (47)$$

it is clear from both panels of Fig. 7 that χ is strongly overproduced with respect to the observed DM abundance $\Omega h^2 \approx 0.12$ [73]. Moreover, the freeze-out temperatures are smaller than $\mathcal{O}(1)$

MeV which means that any new physics contribution invoked to deplete χ is strongly constrained by BBN considerations.

The freeze-out also occurs for $m_\chi = 10$ MeV and $y_\chi = 10^{-4}$ (red line in the left panel). In this case, initially, the interaction between χ and the SM is not sufficiently strong to follow the sudden change of Y_χ^{eq} which is induced by a rapid change of SM degrees of freedom present in the thermal bath at $T = \mathcal{O}(10 - 100)$ MeV. However, Y_χ eventually reaches the equilibrium value and the freeze-out occurs leaving χ with even larger abundance than in the previously discussed scenarios. For $m_\chi = 100$ MeV and $y_\chi = 10^{-4}$ (red line in the right panel) as well as for both cases with $y_\chi = 10^{-5}$, χ does not reach equilibrium. This means that the production occurs via “freeze-in” [74] where the weak interaction with the SM bath leads to a gradual accumulation of χ abundance. From Fig. 7 it is obvious that the final Y_χ in all “freeze-in” scenarios is chiefly set by the initial condition (non-vanishing Y_χ at QCD phase transition) and the freeze-in contribution yields only a subdominant effect.

Even though the DM abundance is still too large, in the “freeze-in” scenarios where χ is not in thermal equilibrium at $\mathcal{O}(1)$ MeV temperatures, a late-time entropy injection episode below T_{QCD} can reduce the χ abundance significantly. Such entropy injection can be achieved for instance via decays of heavy scalars into the states in the thermal bath (see Ref. [31] and references therein). It is clear that Y_χ needs to be diluted by $\mathcal{O}(10^4 - 10^5)$ in order to meet observation. Let us note that alternatives with respect to late-time entropy injection have also been considered. For instance, a heavier, overproduced particle could decay into lighter states which may be DM [75, 76]. This helps because, as may be inferred from Eq. (47), the abundance of DM is proportional to the mass of a DM particle. A detailed analysis of such a scenario is beyond the scope of this project as it would require a significant extension of the Boltzmann equations given in Eq. (46). In such extension, the late-time entropy injection would be avoided. We also note that there may be more models in which MeV-scale particle is produced in right amounts, without a necessity for late-time entropy injection.

In conclusion, for the couplings that can be probed in CONUS or COHERENT ($y_\chi \sim [10^{-5}, 10^{-4}]$), we explored whether in our model χ can be DM, i.e. produced in right amounts in the early Universe. It turns out (see again Fig. 7) that this is not achievable without extending the minimal model presented in Section III. Namely, we find that a late time entropy injection episode is necessary to sufficiently deplete the abundance of χ and render it a viable DM candidate.

Since χ in our model does not scatter on nuclei and electrons at tree-level, the bounds from direct detection are not strong. Moreover, for the considered range of couplings and masses, the $\text{CE}\nu\text{NS}$ cross section is several orders of magnitude smaller than those that can be currently tested at direct DM detection facilities for MeV-scale DM [77]. Given the absence of the annihilation channel into e^+e^- pairs, the constraints from CMB [78] are also not probing the parameter space to which $\text{CE}\nu\text{NS}$ experiments are sensitive.

V. SUMMARY AND CONCLUSIONS

Coherent neutrino-nucleus scattering is a new window to probe physics within and beyond the Standard Model. We have noted here that the final state fermion does not necessarily have to be a light active neutrino. Instead, we have entertained the possibility that an MeV-scale fermion χ is produced in the process, which will lead to a significant modification of the observable recoil spectrum. We have set limits on the parameters that are involved when the interaction of the neutrino- χ pair with quarks is mediated by a light scalar.

The measurable couplings are well compatible with neutrino mass generation via low-scale type-I seesaw mechanism where, interestingly, both χ and the newly introduced GeV-scale fermion N_R

can contribute. Furthermore, χ may be the DM particle, which we have shown to be typically requiring an injection of entropy in the early Universe after the QCD phase transition. Such an entropy injection can be achieved by introducing a new scalar which decays to the states in the thermal bath at late times, diluting the dark matter to the abundance which is in accord with present observations.

Thus, exotic physics in coherent neutrino-nucleus scattering has a variety of interesting implications in neutrino physics and cosmology. The present analysis is only one example of the exciting prospects that this new window to physics has given us the opportunity to probe.

ACKNOWLEDGMENTS

We would like to thank Giorgio Arcadi, Yasaman Farzan, Rasmus S.L. Hansen and Stefan Vogl for useful discussions. WR is supported by the DFG with grant RO 2516/7-1 in the Heisenberg program.

-
- [1] **COHERENT Collaboration**, D. Akimov *et al.*, *Observation of Coherent Elastic Neutrino-Nucleus Scattering*, *Science* **357** (2017), no. 6356 1123–1126, [[1708.01294](#)].
 - [2] D. Z. Freedman, *Coherent Neutrino Nucleus Scattering as a Probe of the Weak Neutral Current*, *Phys. Rev.* **D9** (1974) 1389–1392.
 - [3] C. J. Horowitz, K. J. Coakley, and D. N. McKinsey, *Supernova observation via neutrino - nucleus elastic scattering in the CLEAN detector*, *Phys. Rev.* **D68** (2003) 023005, [[astro-ph/0302071](#)].
 - [4] A. Drukier and L. Stodolsky, *Principles and applications of a neutral-current detector for neutrino physics and astronomy*, *Phys. Rev. D* **30** (Dec, 1984) 2295–2309.
 - [5] A. J. Anderson, J. M. Conrad, E. Figueroa-Feliciano, C. Ignarra, G. Karagiorgi, K. Scholberg, M. H. Shaevitz, and J. Spitz, *Measuring active-to-sterile neutrino oscillations with neutral current coherent neutrino-nucleus scattering*, *Phys. Rev. D* **86** (Jul, 2012) 013004.
 - [6] B. Dutta, Y. Gao, A. Kubik, R. Mahapatra, N. Mirabolfofathi, L. E. Strigari, and J. W. Walker, *Sensitivity to oscillation with a sterile fourth generation neutrino from ultralow threshold neutrino-nucleus coherent scattering*, *Phys. Rev. D* **94** (Nov, 2016) 093002.
 - [7] T. S. Kosmas, D. K. Papoulias, M. Tortola, and J. W. F. Valle, *Probing light sterile neutrino signatures at reactor and Spallation Neutron Source neutrino experiments*, *Phys. Rev.* **D96** (2017), no. 6 063013, [[1703.00054](#)].
 - [8] B. Dutta, R. Mahapatra, L. E. Strigari, and J. W. Walker, *Sensitivity to Z-prime and nonstandard neutrino interactions from ultralow threshold neutrino-nucleus coherent scattering*, *Phys. Rev.* **D93** (2016), no. 1 013015, [[1508.07981](#)].
 - [9] P. B. Denton, Y. Farzan, and I. M. Shoemaker, *A Plan to Rule out Large Non-Standard Neutrino Interactions After COHERENT Data*, *JHEP* **07** (2018) 037, [[1804.03660](#)].
 - [10] M. Lindner, W. Rodejohann, and X.-J. Xu, *Coherent Neutrino-Nucleus Scattering and new Neutrino Interactions*, *JHEP* **03** (2017) 097, [[1612.04150](#)].
 - [11] P. Coloma, M. C. Gonzalez-Garcia, M. Maltoni, and T. Schwetz, *COHERENT Enlightenment of the Neutrino Dark Side*, *Phys. Rev.* **D96** (2017), no. 11 115007, [[1708.02899](#)].
 - [12] J. Liao and D. Marfatia, *COHERENT constraints on nonstandard neutrino interactions*, *Phys. Lett.* **B775** (2017) 54–57, [[1708.04255](#)].
 - [13] D. K. Papoulias and T. S. Kosmas, *COHERENT constraints to conventional and exotic neutrino physics*, *Phys. Rev.* **D97** (2018), no. 3 033003, [[1711.09773](#)].
 - [14] Y. Farzan, M. Lindner, W. Rodejohann, and X.-J. Xu, *Probing neutrino coupling to a light scalar with coherent neutrino scattering*, *JHEP* **05** (2018) 066, [[1802.05171](#)].
 - [15] M. Abdullah, J. B. Dent, B. Dutta, G. L. Kane, S. Liao, and L. E. Strigari, *Coherent elastic neutrino nucleus scattering as a probe of a Z' through kinetic and mass mixing effects*, *Phys. Rev.* **D98** (2018), no. 1 015005, [[1803.01224](#)].

- [16] J. Billard, J. Johnston, and B. J. Kavanagh, *Prospects for exploring New Physics in Coherent Elastic Neutrino-Nucleus Scattering*, [1805.01798](#).
- [17] A. Dodd, E. Papaageorgiu, and S. Ranfone, *The effect of a neutrino magnetic moment on nuclear excitation processes*, *Physics Letters B* **266** (1991), no. 3 434 – 438.
- [18] T. S. Kosmas, O. G. Miranda, D. K. Papoulias, M. Tórtola, and J. W. F. Valle, *Probing neutrino magnetic moments at the spallation neutron source facility*, *Phys. Rev. D* **92** (Jul, 2015) 013011.
- [19] E. Akhmedov, G. Arcadi, M. Lindner, and S. Vogl, *Coherent scattering and macroscopic coherence: Implications for neutrino, dark matter and axion detection*, [1806.10962](#).
- [20] W. Maneschg, “The status of conus.” <https://doi.org/10.5281/zenodo.1286927>, June, 2018.
- [21] R. Strauss *et al.*, *The ν -cleus experiment: A gram-scale fiducial-volume cryogenic detector for the first detection of coherent neutrino-nucleus scattering*, *Eur. Phys. J.* **C77** (2017) 506, [[1704.04320](#)].
- [22] **CONNIE Collaboration**, A. Aguilar-Arevalo *et al.*, *The CONNIE experiment*, *J. Phys. Conf. Ser.* **761** (2016), no. 1 012057, [[1608.01565](#)].
- [23] **MINER Collaboration**, G. Agnolet *et al.*, *Background Studies for the MINER Coherent Neutrino Scattering Reactor Experiment*, *Nucl. Instrum. Meth.* **A853** (2017) 53–60, [[1609.02066](#)].
- [24] H. T. Wong, *Neutrino-nucleus coherent scattering and dark matter searches with sub-keV germanium detector*, *Nucl. Phys.* **A844** (2010) 229C–233C.
- [25] V. Belov *et al.*, *The ν GeN experiment at the Kalinin Nuclear Power Plant*, *JINST* **10** (2015), no. 12 P12011.
- [26] J. Billard *et al.*, *Coherent Neutrino Scattering with Low Temperature Bolometers at Chooz Reactor Complex*, *J. Phys.* **G44** (2017), no. 10 105101, [[1612.09035](#)].
- [27] E. Bertuzzo, C. J. Caniu Barros, and G. Grilli di Cortona, *MeV Dark Matter: Model Independent Bounds*, *JHEP* **09** (2017) 116, [[1707.00725](#)].
- [28] Y. Hochberg, Y. Kahn, M. Lisanti, K. M. Zurek, A. G. Grushin, R. Ilan, S. M. Griffin, Z.-F. Liu, S. F. Weber, and J. B. Neaton, *Detection of sub-MeV Dark Matter with Three-Dimensional Dirac Materials*, *Phys. Rev.* **D97** (2018), no. 1 015004, [[1708.08929](#)].
- [29] M. J. Dolan, F. Kahlhoefer, and C. McCabe, *Directly detecting sub-GeV dark matter with electrons from nuclear scattering*, *Phys. Rev. Lett.* **121** (2018), no. 10 101801, [[1711.09906](#)].
- [30] M. Hufnagel, K. Schmidt-Hoberg, and S. Wild, *BBN constraints on MeV-scale dark sectors. Part I. Sterile decays*, *JCAP* **1802** (2018) 044, [[1712.03972](#)].
- [31] M. Dutra, M. Lindner, S. Profumo, F. S. Queiroz, W. Rodejohann, and C. Siqueira, *MeV Dark Matter Complementarity and the Dark Photon Portal*, *JCAP* **1803** (2018) 037, [[1801.05447](#)].
- [32] A. Berlin, D. Hooper, G. Krnjaic, and S. D. McDermott, *Severely Constraining Dark Matter Interpretations of the 21-cm Anomaly*, *Phys. Rev. Lett.* **121** (2018), no. 1 011102, [[1803.02804](#)].
- [33] R. Mertig, M. Bohm, and A. Denner, *FEYN CALC: Computer algebraic calculation of Feynman amplitudes*, *Comput. Phys. Commun.* **64** (1991) 345–359.
- [34] V. Shtabovenko, R. Mertig, and F. Orellana, *New Developments in FeynCalc 9.0*, *Comput. Phys. Commun.* **207** (2016) 432–444, [[1601.01167](#)].
- [35] P. Coloma, P. B. Denton, M. C. Gonzalez-Garcia, M. Maltoni, and T. Schwetz, *Curtailing the Dark Side in Non-Standard Neutrino Interactions*, *JHEP* **04** (2017) 116, [[1701.04828](#)].
- [36] P. Huber, *On the determination of anti-neutrino spectra from nuclear reactors*, *Phys. Rev.* **C84** (2011) 024617, [[1106.0687](#)]. [Erratum: *Phys. Rev.*C85,029901(2012)].
- [37] T. A. Mueller *et al.*, *Improved Predictions of Reactor Antineutrino Spectra*, *Phys. Rev.* **C83** (2011) 054615, [[1101.2663](#)].
- [38] **TEXONO Collaboration**, S. Kerman, V. Sharma, M. Deniz, H. T. Wong, J. W. Chen, H. B. Li, S. T. Lin, C. P. Liu, and Q. Yue, *Coherency in Neutrino-Nucleus Elastic Scattering*, *Phys. Rev.* **D93** (2016), no. 11 113006, [[1603.08786](#)].
- [39] V. I. Kopeikin, *Flux and spectrum of reactor antineutrinos*, *Phys. Atom. Nucl.* **75** (2012) 143–152. [*Yad. Fiz.*75N2,165(2012)].
- [40] C. Buck, A. P. Collin, J. Haser, and M. Lindner, *Investigating the Spectral Anomaly with Different Reactor Antineutrino Experiments*, *Phys. Lett.* **B765** (2017) 159–162, [[1512.06656](#)].
- [41] C. Giunti, *Precise determination of the ^{235}U reactor antineutrino cross section per fission*, *Phys. Lett.* **B764** (2017) 145–149, [[1608.04096](#)].
- [42] P. Huber, *NEOS Data and the Origin of the 5 MeV Bump in the Reactor Antineutrino Spectrum*, *Phys. Rev. Lett.* **118** (2017), no. 4 042502, [[1609.03910](#)].

- [43] G. Rich, “The coherent collaboration and the first observation of coherent elastic neutrino-nucleus scattering.” <https://doi.org/10.5281/zenodo.1286967>, June, 2018.
- [44] J. H. Chang, R. Essig, and S. D. McDermott, *Supernova 1987A Constraints on Sub-GeV Dark Sectors, Millicharged Particles, the QCD Axion, and an Axion-like Particle*, *JHEP* **09** (2018) 051, [[1803.00993](#)].
- [45] S. Davidson, S. Hannestad, and G. Raffelt, *Updated bounds on millicharged particles*, *JHEP* **05** (2000) 003, [[hep-ph/0001179](#)].
- [46] R. Foot, *Dissipative dark matter explains rotation curves*, *Phys. Rev.* **D91** (2015), no. 12 123543, [[1502.07817](#)].
- [47] L. Wolfenstein, *Neutrino Oscillations in Matter*, *Phys.Rev.* **D17** (1978) 2369–2374.
- [48] S. P. Mikheev and A. Yu. Smirnov, *Resonance Amplification of Oscillations in Matter and Spectroscopy of Solar Neutrinos*, *Sov. J. Nucl. Phys.* **42** (1985) 913–917. [*Yad. Fiz.*42,1441(1985)].
- [49] S. P. Mikheev and A. Yu. Smirnov, *Resonant amplification of neutrino oscillations in matter and solar neutrino spectroscopy*, *Nuovo Cim.* **C9** (1986) 17–26.
- [50] C. A. Argelles, V. Brdar, and J. Kopp, *Production of keV Sterile Neutrinos in Supernovae: New Constraints and Gamma Ray Observables*, [1605.00654](#).
- [51] R. N. Mohapatra and G. Senjanović, *Neutrino mass and spontaneous parity nonconservation*, *Phys. Rev. Lett.* **44** (Apr, 1980) 912–915.
- [52] P. Minkowski, $\mu \rightarrow e\gamma$ at a rate of one out of 109 muon decays?, *Physics Letters B* **67** (1977), no. 4 421 – 428.
- [53] M. Gell-Mann, P. Ramond, and R. Slansky, *Complex Spinors and Unified Theories*, *Conf. Proc.* **C790927** (1979) 315–321, [[1306.4669](#)].
- [54] T. Yanagida, *Horizontal Symmetry and Masses of Neutrinos*, *Conf. Proc.* **C7902131** (1979) 95–99.
- [55] A. Atre, T. Han, S. Pascoli, and B. Zhang, *The Search for Heavy Majorana Neutrinos*, *JHEP* **05** (2009) 030, [[0901.3589](#)].
- [56] A. de Gouvea and A. Kobach, *Global Constraints on a Heavy Neutrino*, *Phys. Rev.* **D93** (2016), no. 3 033005, [[1511.00683](#)].
- [57] F. F. Deppisch, P. S. Bhupal Dev, and A. Pilaftsis, *Neutrinos and Collider Physics*, *New J. Phys.* **17** (2015), no. 7 075019, [[1502.06541](#)].
- [58] A. C. Vincent, E. F. Martinez, P. Hernandez, M. Lattanzi, and O. Mena, *Revisiting cosmological bounds on sterile neutrinos*, *JCAP* **1504** (2015), no. 04 006, [[1408.1956](#)].
- [59] G. Bernardi *et al.*, *Search for Neutrino Decay*, *Phys. Lett.* **166B** (1986) 479–483.
- [60] **DUNE Collaboration**, R. Acciarri *et al.*, *Long-Baseline Neutrino Facility (LBNF) and Deep Underground Neutrino Experiment (DUNE)*, [1601.05471](#).
- [61] O. Lantwin, *Search for new physics with the SHiP experiment at CERN*, *PoS EPS-HEP2017* (2017) 304, [[1710.03277](#)].
- [62] J. L. Feng, I. Galon, F. Kling, and S. Trojanowski, *ForwArd Search ExpeRiment at the LHC*, *Phys. Rev.* **D97** (2018), no. 3 035001, [[1708.09389](#)].
- [63] J. L. Feng, I. Galon, F. Kling, and S. Trojanowski, *Dark Higgs bosons at the ForwArd Search ExpeRiment*, *Phys. Rev.* **D97** (2018), no. 5 055034, [[1710.09387](#)].
- [64] F. Kling and S. Trojanowski, *Heavy Neutral Leptons at FASER*, *Phys. Rev.* **D97** (2018), no. 9 095016, [[1801.08947](#)].
- [65] **NA62 Collaboration**, E. Cortina Gil *et al.*, *Search for heavy neutral lepton production in K^+ decays*, *Phys. Lett.* **B778** (2018) 137–145, [[1712.00297](#)].
- [66] D. Curtin *et al.*, *Long-Lived Particles at the Energy Frontier: The MATHUSLA Physics Case*, [1806.07396](#).
- [67] Z. Xing and S. Zhou, *Neutrinos in Particle Physics, Astronomy and Cosmology*. Advanced Topics in Science and Technology in China. Springer Berlin Heidelberg, 2011.
- [68] P. deNiverville, M. Pospelov, and A. Ritz, *Light new physics in coherent neutrino-nucleus scattering experiments*, *Phys. Rev.* **D92** (2015), no. 9 095005, [[1505.07805](#)].
- [69] S.-F. Ge and I. M. Shoemaker, *Constraining Photon Portal Dark Matter with Texono and Coherent Data*, [1710.10889](#).
- [70] M. Garny, J. Heisig, B. Llf, and S. Vogl, *Coannihilation without chemical equilibrium*, *Phys. Rev.* **D96** (2017), no. 10 103521, [[1705.09292](#)].
- [71] J. Ellis, F. Luo, and K. A. Olive, *Gluino Coannihilation Revisited*, *JHEP* **09** (2015) 127, [[1503.07142](#)].

- [72] P. Gondolo and G. Gelmini, *Cosmic abundances of stable particles: Improved analysis*, *Nucl. Phys.* **B360** (1991) 145–179.
- [73] **Planck Collaboration**, N. Aghanim *et al.*, *Planck 2018 results. VI. Cosmological parameters*, [1807.06209](#).
- [74] L. J. Hall, K. Jedamzik, J. March-Russell, and S. M. West, *Freeze-In Production of FIMP Dark Matter*, *JHEP* **03** (2010) 080, [[0911.1120](#)].
- [75] E. Molinaro, C. E. Yaguna, and O. Zapata, *FIMP realization of the scotogenic model*, *JCAP* **1407** (2014) 015, [[1405.1259](#)].
- [76] S. Baumholzer, V. Brdar, and P. Schwaller, *The New ν MSM ($\nu\nu$ MSM): Radiative Neutrino Masses, keV-Scale Dark Matter and Viable Leptogenesis with sub-TeV New Physics*, *JHEP* **08** (2018) 067, [[1806.06864](#)].
- [77] R. Essig, M. Fernandez-Serra, J. Mardon, A. Soto, T. Volansky, and T.-T. Yu, *Direct Detection of sub-GeV Dark Matter with Semiconductor Targets*, *JHEP* **05** (2016) 046, [[1509.01598](#)].
- [78] T. R. Slatyer, *Indirect dark matter signatures in the cosmic dark ages. I. Generalizing the bound on s-wave dark matter annihilation from Planck results*, *Phys. Rev.* **D93** (2016), no. 2 023527, [[1506.03811](#)].